Macromolecules

Volume 36, Number 21 October 21, 2003

Communications to the Editor

Model for Pattern Formation in Polymer Surfactant Nanodroplets

J. G. E. M. Fraaije* and G. J. A. Sevink

Soft Condensed Matter Group, Leiden Institute of Chemistry, Leiden University, PO Box 9502, 2300 RA Leiden, The Netherlands

Received May 24, 2002
Revised Manuscript Received September 1, 2003

Through self-consistent-field simulation we discovered remarkable bicontinuous structures in dispersed droplets of polymer surfactant (Figures 1 and 2). The nanodroplet structures are soft and fragile: the molecular bonding energy is weak, derived from self-assembly of polymer molecules. Polymer surfactant assemblies have many applications in soft nanotechnology, drug delivery, templates for heterogeneous catalysts, aerosols, and personal care products. Patterned nanostructures are the key in all these applications, and a better understanding of their formation is of paramount interest. In the calculations, we generate the structures by quenching a homogeneous droplet of polymer surfactant in an aqueous bath and then relax the structure by a dynamic variant of self-consistent-field theory. The free energy model is that for a necklace of beads in a mean-field environment:

$$F = -kT \ln \phi - \sum_I \int_V \mathrm{d}\mathbf{r}\, U_I(\mathbf{r})\, \rho_I(\mathbf{r}) + F_{\mathrm{MF}} \qquad (1)$$

where ϕ is the partition function for a mixture of Gaussian chains and solvent, U_I is the external potential conjugate to the particle density ρ_I, and F_{MF} is the mean-field free energy (see Appendix). The minimization of the free energy is by dynamic iteration, adapted from the external potential dynamics algorithm for collective

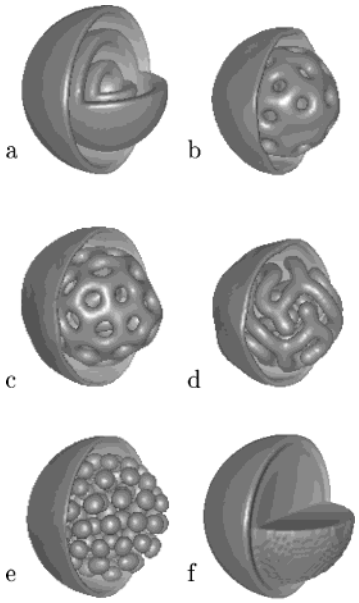

Figure 1. Morphologies of $A_{N-M}B_M$ polymer surfactant nanodroplets (isosurfaces partly removed for visualization). Solvophobic A concentration field for different block ratios $f = M/N$. 0.35 (a), 0.30 (b), 0.25 (c), 0.20 (d), 0.15 (e), 0.10 (f).

Rouse dynamics we proposed before.[1] The dynamic equations are

$$\frac{\partial \rho_I}{\partial \tau} = \nabla^2[\rho_I - f_I(\mu_{\mathrm{MF}})] \qquad (2)$$

where $f_I \equiv -kT\, \delta \ln \phi / \delta U_I$ is the density functional of the polymer (or solvent) molecule, with the mean-field chemical potentials $\mu_{\mathrm{MF},I} \equiv \delta F_{\mathrm{MF}}/\delta \rho_I$ as variables. It can be shown that the density dynamics equations have the same kinetic coefficients as collective Rouse dynamics, which is proper for the spinodal-like microphase separation internal to the droplets.[2] As a technical note, the algorithm is fully explicit in the concentration variables and thereby avoids calculation of the external potentials.

* Corresponding author.

10.1021/ma025559t CCC: $25.00
Published on Web 09/18/2003

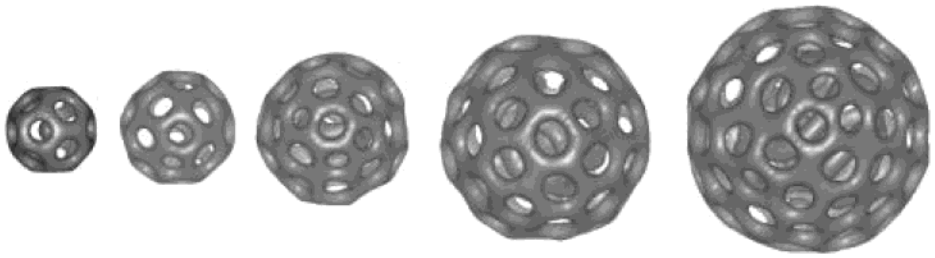

Figure 2. Morphologies of $A_{N-M}B_M$ polymer surfactant nanodroplet ($f = M/N = 0.25$) for different initial radii R^0. From left to right: $R^0 = 20, 23, 26, 30, 33$ (in units of polymer bead size). Notice that in this viewing mode the outer fuzzy shell is not visible.

The simulation parameters are for diblock polymer surfactant $A_{N-M}B_M$ with $N = 20$ in weakly selective solvent and mild segregation, $\chi_{AS} = 1.7$, $\chi_{AB}N = 40$, and $\chi_{AS} - \chi_{BS} = 0.3$, so that A is slightly more solvophobic and B slightly more solvophilic. These are essentially the parameters we verified before by comparison with experimental microphase diagrams of concentrated poly(propylene oxide)−poly(ethylene oxide) aqueous solutions in ambient conditions,[3] in which case each bead or statistical unit corresponds to 3−4 monomers. One should realize that in the mean-field model any polymer surfactant solution with the same properly scaled interaction parameters will behave in exactly the same way.

The free energy model is that for an *nVT* ensemble, and accordingly we do not calculate the global equilibrium in an open system, but rather a local equilibrium morphology of an isolated droplet. The situation is analogous to that of the classic study of the shape of an isolated lipid vesicle, when interactions between vesicles are less relevant. With the selected values of the Flory−Huggins parameters, and N and M, the polymers are all insoluble; hence, the deformations of the droplets are at constant mass of polymer.

The simulations proceed by a sudden quench of a homogeneous droplet in a solvent bath. Following the quench, the droplet takes up or releases additional solvent locally and globally, depending on the particular morphology being formed. The polymer concentration outside the droplet is zero, and this remains so during the morphology adaptation. The simulations are stopped when the order parameters do not change any more: the free energy is then steady in a minimum, and the pattern is a solution to the self-consistent-field condition $\rho_I = f_I$. We have found it advantageous to add a small uncorrelated white noise field to the mean-field chemical potentials. The uncorrelated noise does not obey the fluctuation−dissipation theorem, but it helps small barrier crossings in the free energy landscape. The droplets (initial radius R^0 cell units, each cell has the size of the statistical unit) are placed in the center of the box with sufficient space, $N/2$ cells, between the droplet surface and the boundaries of the computational box, thereby avoiding artifacts resulting from the periodic boundary conditions. In all cases the droplets develop an outer fuzzy layer of the solvophilic B block, but since the confinement of the polymers is soft, the droplet surface is not necessarily spherical. The surface topography is that of small valleys, ridges, and bumps, reflecting the underlying morphology, very much like earth's topography is an image of deeper events. The internal structures, shown in Figure 1, depend on the size ratio $f = M/N$ similar to bulk block copolymer systems. More symmetric polymers $f = 0.35$ form into an onion structure of alternating A and B layers (Figure 1a); slightly less symmetric polymers $f = 0.30-0.25$ form a bicontinuous phase (Figure 1b,c) and then at $f = 0.20$ a cylindrical phase (Figure 1d) and an inverted micellar phase (Figure 1e) at $f = 0.15$. Too asymmetric polymers $f = 0.1$ do not form any internal structure (Figure 1f). In equilibrium the droplets contain an appreciable amount of solvent (ca. 15%), distributed inhomogeneously over the solvophobic A and solvophilic B-rich layers.

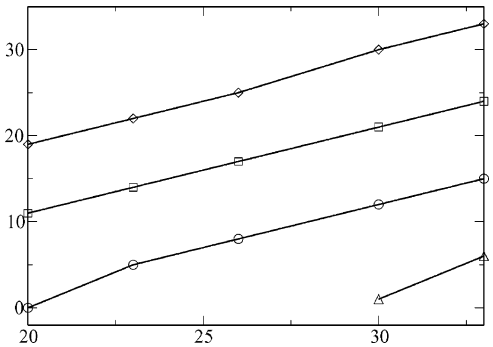

Figure 3. Shell position vs initial radius for different layers.

In the case of $f = 0.25$ (Figure 2), the layers are perforated with pores, and the entire structure is bicontinuous. The droplet strikingly resembles a buckyball, within each inner layer a mixed pore pattern of pentagons, hexagons, and septagons. In bulk solution or melt systems, perforated lamellae consist ideally of a perfectly hexagonal array of pores. In the curved nanodroplets, by rule of geometry, a perfect array of hexagons is impossible to form, and the perforation is mixed. In bulk, a mixture of 85% of this particular polymer surfactant and 15% solvent forms a gyroid bicontinuous structure (data not shown).

From Figure 3, where the radial positions of internal maxima of A concentration are plotted as a function of initial droplet size R^0, it can be observed that, with increasing R^0, the position of the A shells shifts linearly. When an additional layer can be formed, the inner layers move outward. Since the domain size is constant, the pore density in each layer is constant too, and the number of pores in each shell is determined from its radius. There is no intrinsic magic "60" number, as in C_{60}, associated with additional stability of the nanodroplets. The resemblance with a carbon buckyball is purely coincidental on the basis of a geometrical rule for packing pores in a spherical shell.

One may consider several experimental methods for generating the structures—similar as in studies of lipid aggregates—for example by dispersing insoluble polymer surfactant through sonification or through destabilizing a suitable surface film. Perforated lamellar or similar bicontinuous structures have been observed experimentally in thin polymer films[4] and in simulations of

confined systems.[5] Isolated, closed block copolymer membrane structures in solution (polymersomes) are found in various systems.[6,7] In solutions of crew-cut amphiphilic polymers, Eisenberg and co-workers have determined a entire wonderland of structures.[8] Some exhibit onion phases, and others are bicontinuous. The raspberry droplets with the inverted micelles (Figure 1e) resemble so-called large compound vesicles. The agreement at this point is qualitative, in particular regarding the difficult question whether such systems are in local or global equilibrium—the answer depends on the actual formation process. Eisenberg prepares his systems by a very slow quench from good solvent, with demonstrated exchange between different aggregates through fission and fusion phenomena.[6] The recently discovered high-genus giant superstructures ($\gg 1\ \mu$m)[9] have striking resemblance to the bicontinuous droplets. But in our case the pores have size of the polymer coil, whereas in the superstructures the domains apparently are much larger than the constituting polymers. A more detailed comparison, using realistic experimental parameters and calculation of the optimal droplet structure in an open system, is in progress: marvelous structures abound.

Acknowledgment. The supercomputer resources were provided by the High-Performance Computing Centre, University of Groningen. We thank Adi Eisenberg for stimulating discussions.

Appendix. Details of the Free Energy.

The free energy functional $F[\rho]$ (eq 1 in the text) is[1,3]

$$F[\rho] = -kT \ln \frac{\Phi_{\mathrm{p}}^{n_{\mathrm{p}}} \Phi_{\mathrm{W}}^{n_{\mathrm{W}}}}{n_{\mathrm{p}}!\, n_{\mathrm{W}}!} - \sum_I \int_V \mathrm{d}\mathbf{r}\ U_I(\mathbf{r})\, \rho_I(\mathbf{r}) + F_{\mathrm{MF}}[\rho] \tag{A1}$$

Here Φ is the intramolecular partition function for the ideal Gaussian chains in the external field U_I, V is the system volume, n_{p} (n_{W}) is the number of polymer (water) molecules, and $F_{\mathrm{MF}}[\rho]$ is the mean-field contribution due to the nonideal interactions. The mean-field free energy is

$$F_{\mathrm{MF}}[\rho] = \frac{1}{2}\sum_{I,J} \int_V \int_V \mathrm{d}\mathbf{r}\ \mathrm{d}\mathbf{r}'\ \epsilon_{IJ}(|\mathbf{r} - \mathbf{r}'|)\, \rho_I(\mathbf{r})\, \rho_J(\mathbf{r}') + \frac{\kappa}{2} \int_V \mathrm{d}\mathbf{r}\ \Big(\sum_I \nu \rho_I(\mathbf{r}) - 1\Big)^2 \tag{A2}$$

with the mean-field excluded-volume parameter ν, the compressibility parameter κ, and the interaction kernels (with a the bond length)

$$\epsilon_{IJ}(|\mathbf{r} - \mathbf{r}'|) = \epsilon_{IJ}^0 \left(\frac{3}{2\pi a^2}\right)^{3/2} \mathrm{e}^{3(\mathbf{r}-\mathbf{r}')^2/2a^2} \tag{A3}$$

The bare interactions are related to the Flory–Huggins χ-parameters through

$$\chi_{IJ} = \frac{1}{2\nu kT}(\epsilon_{II}^0 + \epsilon_{JJ}^0 - \epsilon_{IJ}^0 - \epsilon_{JI}^0) \tag{A4}$$

The mean-field chemical potential is

$$\mu_{\mathrm{MF},I}[\rho](\mathbf{r}) = \sum_J \int \mathrm{d}\mathbf{r}'\ \epsilon_{IJ}(|\mathbf{r} - \mathbf{r}'|)\, \rho_J(\mathbf{r}') + \kappa\nu\Big(\sum_I \nu \rho_I(\mathbf{r}) - 1\Big) \tag{A5}$$

The explicit formula for the functional f_I is

$$f_I[X](\mathbf{r}) = \mathcal{N} \sum_s \theta_{Is} \int_{V^N} \mathrm{d}\{\mathbf{R}\}\ \delta(\mathbf{r} - \mathbf{R}_s) \mathrm{e}^{-(H_{\mathrm{id}} + \sum_{s'} X_{s'}(\mathbf{R}_{s'}))/kT} \tag{A6}$$

where $\mathcal{N}$ is a normalization constant, θ_{Is} is 1 if bead s is of type I, and 0 otherwise, the integration is over all coordinates of the chain, H_{id} is the intramolecular Gaussian chain Hamiltonian, and X is the field variable. Notice that in the proposed new density dynamics algorithm the mean-field chemical potential is used as the field variable X, so that now $X_I = \mu_{\mathrm{MF},I}[\rho]$, whereas we used $X_I = U_I$ in the previous algorithms.[1,3]

References and Notes

(1) Maurits, N. M.; Fraaije, J. G. E. M. *J. Chem. Phys.* **1997**, *107*, 5879.
(2) In the notation of ref 1, the external potential dynamics algorithm is obtained by left commutation of mobility and gradient operators $\nabla \cdot P_{IJ} \nabla \mu_J \rightarrow P_{IJ} \nabla^2 \mu_J$. The present density dynamics algorithm is obtained by right commutation $\nabla \cdot P_{IJ} \nabla \mu_J \rightarrow \nabla^2 P_{IJ} \mu_J$, which is valid provided $\mu_J \ll kT$.
(3) van Vlimmeren, B. A. C.; Maurits, N. M.; Zvelindovsky, A. V.; Sevink, G. J. A.; Fraaije, J. G. E. M. *Macromolecules* **1999**, *32*, 646.
(4) Knoll, A.; Horvat, A.; Lyakhova, K. S.; Krausch, G.; Sevink, G. J. A.; Zvelindovsky, A. V.; Magerle, R. *Phys. Rev. Lett.* **2002**, *89*, 035501.
(5) Huinink, H. P.; van Dijk, M. A.; Brokken-Zijp, J. C. M.; Sevink, G. J. A. *Macromolecules* **2001**, *34*, 5325.
(6) Discher, D. E.; Eisenberg, A. *Science* **2002**, *297*, 967.
(7) Discher, B. M.; Won, Y. Y.; Ege, D. S.; Lee, J. C. M.; Bates, F. S.; Discher, D. E.; Hammer, D. A. *Science* **1999**, *284*, 1143.
(8) Cameron, N. S.; Corbiere, M. K.; Eisenberg, A. *Can. J. Chem.* **1999**, *77*, 1311.
(9) Haluska, C. K.; Góźdź, W. J.; Döbereinder, H.-G.; Förster, S.; Gompper, G. *Phys. Rev. Lett.* **2002**, *89*, 238302.

MA025559T